

Gene mutations of esophageal squamous cell carcinoma based on next-generation sequencing

Long Wang¹, Yi-Meng Jia¹, Jing Zuo¹, Yu-Dong Wang¹, Zhi-Song Fan¹, Li Feng¹, Xue Zhang¹, Jing Han¹, Wen-Jing Lyu¹, Zhi-Yu Ni^{2,3}

¹Department of Oncology, The Fourth Hospital of Hebei Medical University, Shijiazhuang, Hebei 050011, China;

²The Affiliated Hospital of Hebei University, Baoding, Hebei 071000, China;

³School of Basic Medical Science, Hebei University, Baoding, Hebei 071000, China.

Abstract

Background: Esophageal squamous cell carcinoma (ESCC) is one of the most aggressive cancers without effective therapy. To explore potential molecular targets in ESCC, we quantified the mutation spectrum and explored the relationship between gene mutation and clinicopathological characteristics and programmed death-ligand 1 (PD-L1) expression.

Methods: Between 2015 and 2019, 29 surgically resected ESCC tissues and adjacent normal tissues from the Fourth Hospital of Hebei Medical University were subjected to targeted next-generation sequencing. The expression levels of PD-L1 were detected by immunohistochemistry. Mutational signatures were extracted from the mutation count matrix by using non-negative matrix factorization. The relationship between detected genomic alterations and clinicopathological characteristics and PD-L1 expression was estimated by Spearman rank correlation analysis.

Results: The most frequently mutated gene was *TP53* (96.6%, 28/29), followed by *NOTCH1* (27.6%, 8/29), *EP300* (17.2%, 5/29), and *KMT2C* (17.2%, 5/29). The most frequently copy number amplified and deleted genes were *CCND1/FGF3/FGF4/FGF19* (41.4%, 12/29) and *CDKN2A/2B* (10.3%, 3/29). By quantifying the contribution of the mutational signatures to the mutation spectrum, we found that the contribution of signature 1, signature 2, signature 10, signature 12, signature 13, and signature 17 was relatively high. Further analysis revealed genetic variants associated with cell cycle, chromatin modification, Notch, and Janus kinase-signal transducer and activator of transcription signaling pathways, which may be key pathways in the development and progression of ESCC. Evaluation of PD-L1 expression in samples showed that 13.8% (4/29) of samples had tumor proportion score $\geq 1\%$. 17.2% (5/29) of patients had tumor mutation burden (TMB) above 10 mut/Mb. All samples exhibited microsatellite stability. TMB was significantly associated with lymph node metastasis ($r = 0.468$, $P = 0.010$), but not significantly associated with PD-L1 expression ($r = 0.246$, $P = 0.198$). There was no significant correlation between PD-L1 expression and detected gene mutations (all $P > 0.05$).

Conclusion: Our research initially constructed gene mutation profile related to surgically resected ESCC in high-incidence areas to explore the mechanism underlying ESCC development and potential therapeutic targets.

Keywords: Esophageal squamous cell carcinoma; Next-generation sequencing; Mutational signature; Programmed death-ligand 1

Introduction

Esophageal squamous cell carcinoma (ESCC) is one of the most common and invasive cancers worldwide, with nearly 79% of ESCC occurring in Asian countries.^[1] The incidence of ESCC had obvious regional characteristics, especially in Hebei province. Although great progress has been made in the traditional treatment of ESCC, the survival rate of patients has not significantly improved. Chinese and Japanese researchers in related fields have revealed the genetic landscape of ESCC in different regions by using next-generation sequencing (NGS), which

provides an important basis for further exploration of the pathogenesis of ESCC and the search for therapeutic targets.^[2-4] In this study, we collected 29 ESCC samples and detected 520 tumor-related genes. The preliminary construction of mutation gene profile related to surgically resected ESCC in high-incidence areas can further complement the genomic research of ESCC in China.

Endogenous (such as spontaneous deamination of 5-methylcytosines) and exogenous (such as ultraviolet radiation) factors cause DNA damage and induce DNA damage repair, leaving genomic imprints that can be detected by sequence analyses. Mutation spectrums

Access this article online

Quick Response Code:



Website:

www.cmj.org

DOI:

10.1097/CM9.0000000000001411

Correspondence to: Prof. Zhi-Yu Ni, The Affiliated Hospital of Hebei University, No. 342 Yuhua East Road, Lianchi District, Baoding, Hebei 071000, China
E-Mail: nizhiyu@hbu.edu.cn

Copyright © 2021 The Chinese Medical Association, produced by Wolters Kluwer, Inc. under the CC-BY-NC-ND license. This is an open access article distributed under the terms of the Creative Commons Attribution-Non Commercial-No Derivatives License 4.0 (CCBY-NC-ND), where it is permissible to download and share the work provided it is properly cited. The work cannot be changed in any way or used commercially without permission from the journal.

Chinese Medical Journal 2021;134(6)

Received: 18-11-2020 Edited by: Pei-Fang Wei

mathematically extracted from these genomic imprints are called mutation signatures. These signatures reflect different genetic perturbations that occur before and during malignant transformation and progression.^[5] Currently, 30 different mutational signatures are published in the Catalogue of Somatic Mutations in Cancer (COSMIC). Previous studies have verified that mutational signature 1 and apolipoprotein B messenger RNA-editing enzyme catalytic polypeptide (APOBEC)-mediated mutational signatures are common mutational signatures in ESCC.^[5,6] However, patients with ESCC have high heterogeneity and complex genomic mutational landscape. In order to further understand the details of complex mutation mechanisms, we quantified the contribution of the mutation spectrum of COSMIC to the sample mutation spectrum.

With the in-depth development of molecular biology, immunotherapy has shown its unique curative effect in advanced ESCC. A multi-center phase Ib/II trial (NCT02915432) showed that 59 patients with advanced refractory ESCC were treated with toripalimab (programmed death-1 [PD-1] inhibitors). Patients without *CCND1/FGF3/FGF4/FGF19* amplification had significantly better objective response rates and progression-free survival than individuals with *CCND1/FGF3/FGF4/FGF19* amplification.^[7] The genomic amplification of *CCND1/FGF3/FGF4/FGF19* may be related to the poor prognosis of immunotherapy. The results of this study provide important ideas for further exploration of the treatment of ESCC, such as improving the accuracy of immunotherapy screening to improve efficacy. However, there are few biomarkers that can accurately predict the effects of immunotherapy. Previous analyses have shown that programmed death-ligand 1 (PD-L1) expression, tumor mutation burden (TMB), and microsatellite instability (MSI) may be biomarkers for the immunotherapy response.^[8-10] Although nivolumab and pembrolizumab (PD-1 inhibitors) are currently used for patients with advanced ESCC, the expression of PD-L1 in patients with resectable ESCC has not been explored, and few researches have been conducted on TMB and the MSI status in ESCC. We used immunohistochemical (IHC) 22C3 technology to detect PD-L1 expression, and further explored the correlation between PD-L1 expression and the detected gene mutation profile which can help to identify the best candidate for immunotherapy. Next-generation sequencing technology to detect TMB and MSI provides a theoretical basis for immunotherapy for patients with resectable ESCC.

Methods

Ethical approval

The study protocol was reviewed and approved by the Ethics Committee of the Fourth Hospital of Hebei Medical University (No. 2017009) and the requirement for written informed consent was waived.

Patients and sample collection

A total of 29 pairs of matched tissues (cancer tissues and adjacent tissues) were obtained from 29 patients with

ESCC who underwent surgical resection between 2015 and 2019 at The Fourth Hospital of Hebei Medical University. Among all patients, there were 16 males and 13 females, the mean age was 62 years (ranging from 51 to 73 years), and the patients with ESCC were at an early clinical stage (tumor, node, and metastasis [TNM] stage: IA-III B). There were nine patients with lesions in the upper segment, 13 patients with lesions in the middle segment, and seven patients with lesions in the lower segment [Supplementary Table 1, <http://links.lww.com/CM9/A476>].

DNA extraction and sequencing

DNA was extracted using QIAamp DNA formalin-fixed paraffin-embedded (FFPE) Tissue Kits (Qiagen, Valencia, CA, USA) according to the manufacturer's instructions. The quality of DNA was evaluated using a NanoDrop™ 8000 (Nanodrop Technologies, Wilmington, DE, USA) and quantified using Qubit double-stranded DNA HS Assay Kits (Invitrogen, Carlsbad, CA, USA) on a Qubit 3.0 Fluorometer (Invitrogen). Shearing, end repair, and ligation were performed on DNA. The DNA fragments with 200 to 400 bp in size were selected with beads (Agencourt AMPure XP Kit; Beckman Coulter, Brea, CA, USA), followed by hybridization with probe baits, selection with magnetic beads, and polymerase chain reaction amplification. The indexed samples were sequenced on a NextSeq 500 sequencer (Illumina, San Diego, CA, USA).

Sequencing data analysis

Burrows-Wheeler aligner 0.7.10 (Dice Holdings, New York, NY, USA) was used to map reads to the human genome (hg19). Genome Analysis Toolkit 3.2 (Broad Institute, Cambridge, MA, USA), Picards (Broad Institute), and VarScan (Sourceforge, Mountain View, CA, USA) were optimized for local comparison, tag repetition, and mutation calling. The VarScan filter pipeline was used to filter the variants and loci with depths less than 100. Insertions or deletions required at least five supported reads, and single nucleotide variants (SNVs) required eight supported reads. A panel of 520 genes which are closely related to cancer mechanisms and targeted therapies were analyzed using probe hybridization to detect the entire exon region of 312 genes and hot spot mutations (exons, introns, and promoter regions) of 208 genes. Aberrations, such as gene mutations, amplifications, and fusions, which had a clear clinical correlation with cancer, were detected in a comprehensive and accurate manner [Supplementary Table 2, <http://links.lww.com/CM9/A476>]. TMB was calculated by adding all of the detected somatic variants and dividing this number by the size of the target region. Gene detection can identify the microsatellite status. The presence of 13 or more microsatellite site errors indicated the MSI-H status. In most MSI-H tumors, but not in MSI-low or microsatellite stable (MSS) tumors, the expression of mismatch repair (MMR) proteins is absent or significantly decreased.

Evaluation of PD-L1 expression

The expression levels of PD-L1 were evaluated by the PD-L1 IHC 22C3 pharmDx assay (Merk, Kenilworth, NJ, USA). The tumor proportion score refers to the percentage

of tumor cells with partial or intact membrane staining in all live tumor cells in the sample.^[11]

Statistical analysis

The R Package Mutational Patterns (<https://doi.org/10.1101/071761>) were used to evaluate and visualize a multitude of mutational patterns in base substitution catalogs. Mutational signatures can be extracted from the mutation count matrix by using non-negative matrix factorization.^[12]

The IBM SPSS Statistics software application (version 24.0; IBM, Armonk, NY, USA) was used for the data analysis. Spearman rank correlation was used to analyze correlations between detected genomic alterations and clinicopathological characteristics and PD-L1 expression. A two-sided *P* value less than 0.05 was considered statistically significant.

Results

High-frequency mutation gene profile of 29 patients with ESCC

Targeted NGS was performed on 29 surgically resected ESCC tissues and adjacent normal tissues using a 520-cancer-gene panel. Among 520 genes closely related to cancer mechanism and targeted therapy, 421 genomic alterations were identified, of which there were 230 SNVs, 35 insertions and deletions (INDELs), 147 copy number amplifications, and nine copy number deletions [Figure 1, Supplementary Table 3, <http://links.lww.com/CM9/A476>]. The most frequently mutated gene was *TP53* (96.6%, 28/29), followed by *NOTCH1* (27.6%, 8/29), *EP300* (17.2%, 5/29), and *KMT2C* (17.2%, 5/29). Comparing the detected mutation sites with those in the COSMIC database, 192 novel mutation sites were discovered, with the *TP53* hotspot mutations, p.R273H, p.R248Q, and p.R175H, in four samples and the *PIK3CA* hotspot mutation, p.H1047L, in one sample.

Copy number variation occurred in 69.0% (20/29) of patients with ESCC. *CCND1/FGF3/FGF4/FGF19*, co-localized on 11q13.3, were co-amplified in The Cancer Genome Atlas database. Among the copy number amplified genes, the *CCND1/FGF3/FGF4/FGF19* gene cluster had the highest frequency (41.4%, 12/29), followed by *NKX2-1* (17.2%, 5/29), *NFKBIA* (13.8%, 4/29), *TP63* (10.3%, 3/29), *IL7R* (10.3%, 3/29), *PGR* (10.3%, 3/29), and *ERBB2* (10.3%, 3/29). The copy number deleted genes were *CDKN2A/2B* (10.3%, 3/29) and *MET* (6.9%, 2/29).

Notably, *NOTCH1* (31.0%, 9/29), *NFKBIA* (20.7%, 6/29), *CDKN2A* (20.7%, 6/29), *TRRAP* (13.8%, 4/29), *PIK3CA* (13.8%, 4/29), *CHD4* (13.8%, 4/29), *DOT1L* (10.3%, 3/29), *FAT3* (10.3%, 3/29), *KDM5A* (10.3%, 3/29), and *KEAP1* (10.3%, 3/29) harbored alterations in at least 10% of the primary tumors.

Mutational signatures of ESCC

The total number of point mutations was 183, and the most common type of mutation was the C>T transition,

followed by C>G and C>A [Figure 2A, Supplementary Table 4, <http://links.lww.com/CM9/A476>]. We extracted four mutational signatures from ESCC with varying mutational activities [Figure 2B, Supplementary Table 5, <http://links.lww.com/CM9/A476>]. The similarities between signatures A–D and each COSMIC signature were calculated [Figure 2C, Supplementary Table 6, <http://links.lww.com/CM9/A476>]. Signatures A–D showed low similarity to any COSMIC signature (the highest cosine similarity was 0.67), which may be due to the limited clinical sample size or novel mutational signatures in ESCC.

In order to further understand the details of the complex mutation mechanism, the contribution of any signature set to the sample mutation spectrum was also quantified. The contribution of signature 1, APOBEC-mediated mutational signatures (signature 2 and signature 13), signature 10, signature 12, and signature 17 was relatively high in all samples (58.6%, 51.7%, 41.4%, 31.0%, and 31.0%, respectively) [Supplementary Table 7, <http://links.lww.com/CM9/A476>]. We noted that two samples showed high similarity to COSMIC signature 1 (cosine similarity 0.76 and 0.71, respectively). Signature 1 was the result of an endogenous mutational process initiated by spontaneous deamination of 5-methylcytosine [Figure 2D, Supplementary Table 8, <http://links.lww.com/CM9/A476>].^[13] Signature 2 was characterized by C>T mutation. One sample was highly similar to COSMIC signature 13 (cosine similarity 0.93). Signature 13, which primarily resulted in the C>G mutation, was related to the increase of the activity of the APOBEC family-mediated mutagenesis.^[14] Signature 10 exhibited strand bias for C>A mutations in the TpCpT context and for T>G mutations in the TpTpT context. Signature 12 exhibited strong transcriptional strand bias for T>C substitutions. The etiology of signature 17 remains unknown. It showed that signature 6 and signature 16 highly contributed to sample 16 and sample 24, respectively [Figure 2E]. Signature 6 was associated with small INDELs (mostly 1 bp) with a large number of single/polynucleotide repeats. Signature 16 was characterized by T>C mutations in the ApTpN context.

Functionally aberrant pathways in ESCC

Cell cycle regulators constituted the most frequently disrupted category, including mutations in *TP53* (96.6%, 28/29), *EP300* (17.2%, 5/29), *CREBBP* (10.3%, 3/29), *STAG2* (10.3%, 3/29), *RB1* (6.9%, 2/29), *PRKDC* (6.9%, 2/29), *ATM* (6.9%, 2/29), *ATR* (6.9%, 2/29), *MYC* (3.4%, 1/29) and amplifications or deletions of *CCND1* (41.4%, 12/29), *CDKN2A/B* (10.3%, 3/29), *CDK6* (6.9%, 2/29), and *CCNE1* (6.9%, 2/29).

Genetic alterations associated with chromatin modification occurred in 79.3% (23/29) of ESCC samples. Components of the SWI/SNF (SWItch/Sucrose Non-Fermentable) complex, including AT-rich interaction domain 1A (*ARID1A*) (4/29, 13.8%), *ATRX* (3/29, 10.3%), *ARID2* (1/29, 3.4%), and *SMARCA4* (1/29, 3.4%), were mutated in ESCC. Four mutations and two amplifications in *CHD4* were identified. *TP63* was amplified in 10.3% (3/29) of ESCC tumors.



Figure 1: High-frequency mutation gene profile of 29 patients with ESCC. The ordinate corresponds to each gene and is sorted according to the mutation frequency of the gene in the sample. The abscissa corresponds to 29 samples of ESCC. The right panel shows the number of mutations in each gene. The top panel shows the number of mutations in each sample. CN_amp: Copy number amplification; CN-del: Copy number deletion; ESCC: Esophageal squamous cell carcinoma; TMB-H: Tumor mutation burden-high; TMB-L: Tumor mutation burden-low.

Genes involved in the Janus kinase-signal transducer and activator of transcription (JAK-STAT) signaling pathway were altered in 75.9% (22/29) of tumors, and included mutations in *JAK1*, *JAK2*, *JAK3*, *STAT3*, and *PIK3CA*. The amplification of *IL7R* was found in 10.3% (3/29) of cases.

Altered genes in the Notch signaling pathway, playing an important role in regulating normal cell differentiation, were mutated in 48.3% (14/29) of cases. *NOTCH1* showed mutations in eight cases. In addition, the

mutations in *CREBBP* and *EP300* were detected in three and five samples, respectively. *NOTCH1* and *NOTCH3* were amplified in 6.9% (2/29) of cases.

Biomarkers to predict the efficacy of immunotherapy

Among 29 samples evaluated for PD-L1 expression, 13.8% (4/29) of samples had TPS \geq 1% [Figure 3A–C]. By performing targeted NGS in 29 ESCC samples, we found the median value of TMB was 5.6 mut/Mb, ranging from 0.8 to 42.9 mut/Mb [Figure 3D]. There were 17.2%

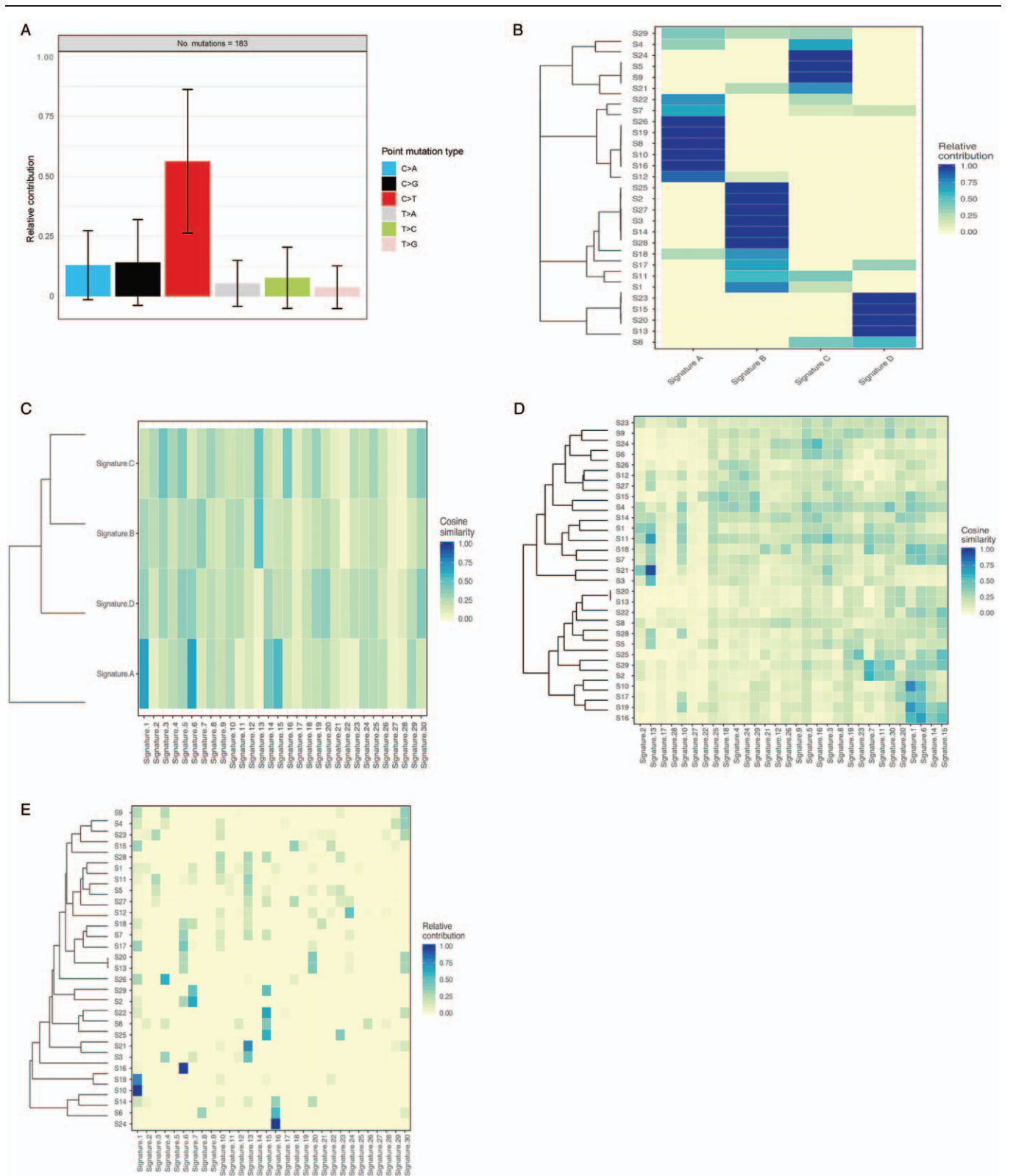


Figure 2: Mutational signatures of ESCC. (A) Point mutation type. Single nucleotide substitutions are divided into six categories. (B) Signature A–D. (C) Pairwise cosine similarity between signature A–D and COSMIC signatures. (D) Cosine similarity between mutational profiles and COSMIC signatures. (E) The contribution of any set of signatures to the mutational profile of a sample can be quantified. COSMIC: Catalogue of somatic mutations in cancer; ESCC: Esophageal squamous cell carcinoma.

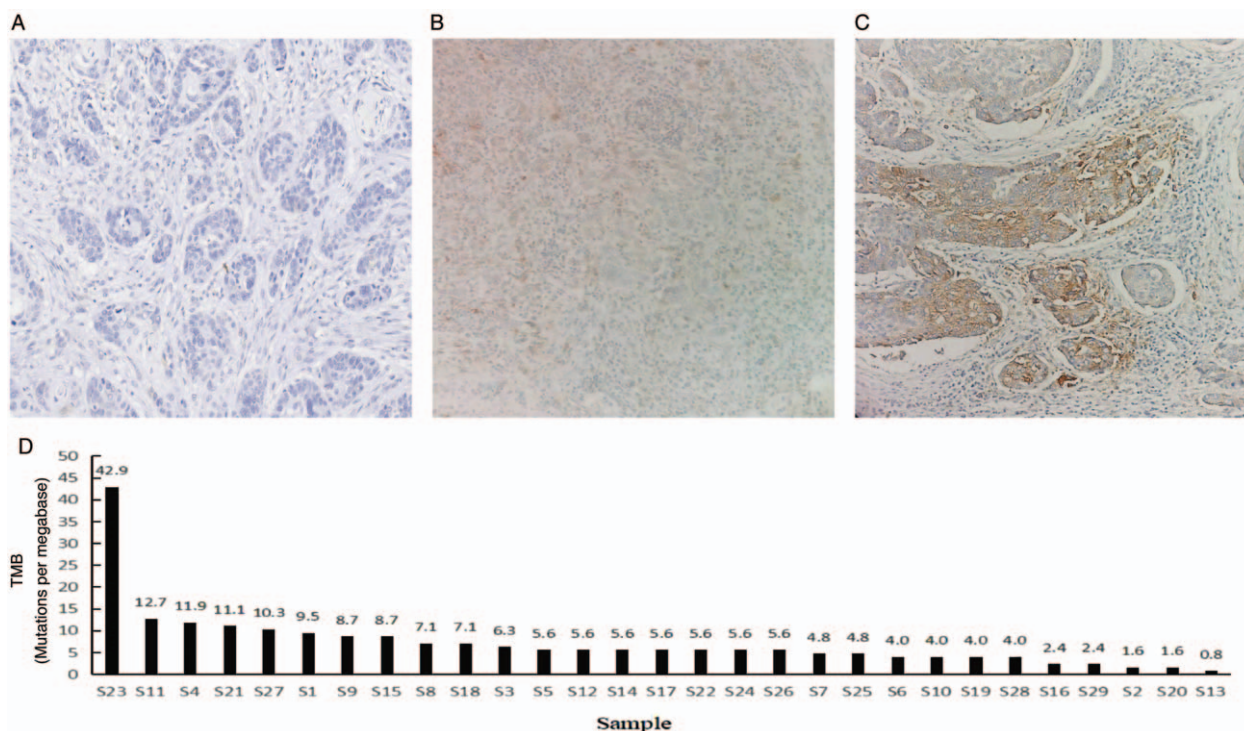


Figure 3: Biomarkers to predict the efficacy of immunotherapy (IHC). (A) Negative expression of PD-L1. Original magnification $\times 200$. (B) PD-L1 TPS = 1%. Original magnification $\times 200$. (C) PD-L1 TPS = 20%. Original magnification $\times 200$. (D) The median value of TMB was 5.6 mut/Mb, ranging from 0.8 to 42.9 mut/Mb. IHC: Immunohistochemistry; mut/Mb: Mutations per megabase; PD-L1: Programmed death-ligand 1; TMB: Tumor mutation burden; TPS: Tumor proportion score.

Table 1: Correlation analysis results between gene mutation and clinicopathological characteristics and PD-L1 expression in 29 esophageal squamous cell carcinoma samples.

Items	Age	Smoking	Drinking	Site	Differentiation	T-stage	N-stage	PD-L1
TMB	0.068	-0.236	-0.256	-0.189	0.230	-0.320	0.468*	0.246
CCND1/FGF3/FGF4/FGF19	0.164	-0.080	-0.362	-0.198	0.165	-0.473 [†]	-0.023	0.042
NOTCH1	0.175	-0.064	-0.081	0.153	0.181	0.074	-0.144	-0.267
CDKN2A	0.010	-0.048	-0.315	0.022	0.024	-0.654 [†]	-0.301	0.025
KMT2D	0.018	0.099	0.201	0.051	0.285	0.043	0.407*	-0.160
NFKBIA	0.363	-0.048	-0.315	-0.175	0.024	-0.339	-0.227	-0.204
ARID1A	-0.222	-0.107	0.201	-0.282	0.139	0.043	0.240	0.110
EP300	0.099	0.019	0.127	0.141	-0.038	0.260	0.067	-0.182

Data are presented as correlation coefficients (r). * $P < 0.05$. [†] $P < 0.01$. ARID1A: AT-rich interaction domain 1A; PD-L1: Programmed death-ligand 1; TMB: Tumor mutation burden.

(5/29) which were higher than 10 mut/Mb. All samples were MSS.

Relationship between gene mutation and clinicopathological characteristics and PD-L1 expression

KMT2D mutations were associated with lymph node metastasis ($r = 0.407, P = 0.028$). CCND1/FGF3/FGF4/FGF19 amplification ($r = -0.473, P = 0.009$) and CDKN2A deletion ($r = -0.654, P < 0.001$) were associated with the depth of infiltration. TMB was associated with lymph node metastasis ($r = 0.468, P = 0.010$), and it was not significantly associated with PD-L1 expression ($r = 0.246, P = 0.198$). PD-L1 expression was not significantly

associated with the detected genetic variations (all $P > 0.05$) [Table 1].

Discussion

Although the traditional treatment methods have made great progress in ESCC, the survival rate of patients has not significantly improved, so exploring the pathogenesis and biological characteristics has become the primary task. We used next-generation sequencing to preliminarily construct mutation gene profile related to surgically resected ESCC in high-incidence areas, and further explored the details of the complex mutation mechanism and biomarkers to

predict the efficacy of immunotherapy, which provides the possibility for developing more precise treatment options.

This study found that the most frequently mutated genes were *TP53*, followed by *NOTCH1*, *EP300*, *KMT2C*, and so on. The most frequently copy number amplified and deleted genes were *CCND1/FGF3/FGF4/FGF19* and *CDKN2A/2B*. This is consistent with the results of a previous study.^[3] Although the sample size of this study is small, this study preliminarily constructed mutation gene profile related to surgically resected ESCC in a high-incidence area of Hebei Province, which can further complement the genomic research of ESCC in China.

The ESCC has high heterogeneity and complex molecular mechanism, and the details of these mechanisms require further exploration. An analysis of mutational signatures could be a promising new tool for molecular tumor diagnosis and classification. In this study, we identified four mutational signatures (signatures A–D) in ESCC. The similarity between mutation signatures A–D and COSMIC mutation signatures was low, and their clinical significance was not clear.

We quantified the contribution of any set of COSMIC signatures to the sample mutation spectrum. Signature 1 and APOBEC-mediated mutational signatures (signature 2 and signature 13) were the most commonly observed signatures in ESCC samples, which is consistent with the previous study.^[5] Lin *et al*^[5] found that patients with APOBEC-mediated mutational signature had more targeted driver genes including *ZNF750*, *PIK3CA*, *MLL2*, *MLL3*, and *RB1*. We also found that signature 10, signature 12, and signature 17 had relatively high contributions. Signature 10, which was previously associated with altered activity of the error-prone *POLE*, generates a massive number of mutations in uterine cancer and colorectal subsets.^[15,16] However, *POLE* was not altered in our samples, which may be related to the low mutational activity of signature 10. Signature 17 is associated with lung adenocarcinoma, breast cancer, B-cell lymphoma, liver cancer, gastric cancer, and melanoma. Signature 17 has been shown to be associated with high neoantigen load, which means that these patients may require immunotherapy.^[17,18] Signature 6 and signature 16 had relatively high contributions in two samples. The signature 6, present in microsatellite unstable tumors, is closely related to the inactivation of the DNA *MMR* gene.^[19] However, the samples with the contribution of signature 6 in our cohort were all MSS. Li *et al*^[4] found that signature 16 was significantly associated with alcohol consumption. The patient linked to sample 24 had a long history of drinking, indicating a possible association between signature 16 and alcohol consumption in ESCC.

Further analysis revealed genetic variants were associated with cell cycle, chromatin modification, Notch and JAK-STAT signaling pathways, which may be key pathways in the development and progression of ESCC.

Genetic alterations in the SWI/SNF complex were induced at an early stage of esophageal squamous cell carcinogenesis.^[20] *ARID1A*, which were detected in 13.8% (4/29) of ESCC samples in the study, is a non-catalytic subunit of the

SWI/SNF chromatin-remodeling complex that regulates gene transcription.^[21,22] *TP63* (10.3%, 3/29) encodes TAp63, which is functionally similar to *TP53* and Δ Np63, which lacks the transcription-activating domain of TAp63, and seems to have strong carcinogenicity.^[23]

EP300 encoding the E1A-binding protein p300 was mutated in 5 samples (5/29, 17.2%), and the incidence was higher than a Japanese study (8.3%).^[2] Cancer-associated histone acetyl transferases (HAT) domain-altering mutations and deletions impair the HAT activity of p300, leading to the hypothesis that p300 and *CREBBP* acetyltransferase activities might be tumor-suppressive.^[24,25]

Effective molecular targeted drugs for ESCC with improved therapeutic efficacy and few adverse reactions are highly anticipated. *CDKN2A* was amplified or mutated in 20.6% of samples in the study. *CDKN2A* is a multifunctional gene that produces p16 and p19 to arrest the cell cycle at the G1/S checkpoint through cyclin-dependent kinases 4/6 (CDK4/6)-regulated mechanism,^[26] and the proteins bind to murine double minute 2 to block the reduction in p53 levels.^[27] CDK4/6 is a potential target in *CDKN2A*-deficient tumors. Palbociclib has already shown efficacy and safety in metastatic liposarcoma.^[28] *CDKN2A* could also be a target for anti-cancer therapy in ESCC.

Traditional anti-tumor strategies have not shown significant survival benefits, which prompted the development of new treatments for patients with ESCC. Immunotherapy showed good efficacy for esophageal cancer, and the commonly used efficacy predictors included PD-L1 and TMB.^[29-32] This study found that TMB is associated with lymph node metastasis and has no significant association with PD-L1 expression, consistent with prior reports.^[33] Singal *et al*^[33] explored the correlation between the genome and clinicopathological characteristics of 4064 patients with non-small cell lung cancer, and found that there was no significant correlation between TMB level and PD-L1 expression. Therefore, PD-L1 and TMB may be two independent biomarkers. However, there are not many studies on TMB in ESCC. The relationship between TMB and PD-L1 still needs to be further explored in large samples.

Exploring the correlation between PD-L1 expression and detected gene mutations can help further understand the carcinogenesis mechanism regulated by PD-L1. Kim *et al*^[34] found that the loss of *ARID1A* was closely related to the high expression of PD-L1 in gastric cancer. In this study, due to the limited sample size, the positive rate of PD-L1 expression was low, and there was no significant correlation between PD-L1 expression and the detected genetic variation. Further expanding the sample size in the future and exploring the correlation between PD-L1 expression and the ESCC will help find the best candidate for immunotherapy.

In this study, the clinical significance of *KMT2D* mutation, *CCND1/FGF3/FGF4/FGF19* amplification, and *CDKN2A* deletion in ESCC progression and metastasis was identified by analyzing the relationship between gene mutation and clinicopathological characteristics. *KMT2D* mutation, *CCND1/FGF3/FGF4/FGF19* amplification, and *CDKN2A*

deletion may be new prognostic factors and therapeutic targets for ESCC.

This study also had some limitations. The sample size was limited. Furthermore, this study was based on selected cancer-related genomes, and we may have missed some important genes or signaling pathways.

In conclusion, our research initially constructed mutation gene profile related to surgically resected ESCC in high-incidence areas, and provided new ideas for precise targeted therapy and precise immunotherapy of ESCC.

Conflicts of interest

None.

References

- Arnold M, Soerjomataram I, Ferlay J, Forman D. Global incidence of oesophageal cancer by histological subtype in 2012. *Gut* 2015;64:381–387. doi: 10.1136/gutjnl-2014-308124.
- Sawada G, Niida A, Uchi R, Hirata H, Shimamura T, Suzuki Y, *et al.* Genomic landscape of esophageal squamous cell carcinoma in a Japanese population. *Gastroenterology* 2016;150:1171–1182. doi: 10.1053/j.gastro.2016.01.035.
- Chang J, Tan W, Ling Z, Xi R, Shao M, Chen M, *et al.* Genomic analysis of oesophageal squamous-cell carcinoma identifies alcohol drinking-related mutation signature and genomic alterations. *Nat Commun* 2017;8:15290. doi: 10.1038/ncomms15290.
- Li XC, Wang MY, Yang M, Dai HJ, Zhang BF, Wang W, *et al.* A mutational signature associated with alcohol consumption and prognostically significantly mutated driver genes in esophageal squamous cell carcinoma. *Ann Oncol* 2018;29:938–944. doi: 10.1093/annonc/mdy011.
- Lin DC, Dinh HQ, Xie JJ, Mayakonda A, Silva TC, Jiang YY, *et al.* Identification of distinct mutational patterns and new driver genes in oesophageal squamous cell carcinomas and adenocarcinomas. *Gut* 2018;67:1769–1779. doi: 10.1136/gutjnl-2017-314607.
- Du P, Huang P, Huang X, Li X, Feng Z, Li F, *et al.* Comprehensive genomic analysis of oesophageal squamous cell carcinoma reveals clinical relevance. *Sci Rep* 2017;7:15324. doi: 10.1038/s41598-017-14909-5.
- Wang F, Ren C, Zhao Q, Xu N, Shen L, Dai GH, *et al.* Association of frequent amplification of chromosome 11q13 in esophageal squamous cell cancer with clinical benefit to immune check point blockade. *J Clin Oncol* 2019;37:4036. doi: 10.1200/JCO.2019.37.15_suppl.4036.
- Le DT, Durham JN, Smith KN, Wang H, Bartlett BR, Aulakh LK, *et al.* Mismatch repair deficiency predicts response of solid tumors to PD-1 blockade. *Science* 2017;357:409–413. doi: 10.1126/science.aan6733.
- Rooney MS, Shukla SA, Wu CJ, Getz G, Hacohen N. Molecular and genetic properties of tumors associated with local immune cytolytic activity. *Cell* 2015;160:48–61. doi: 10.1016/j.cell.2014.12.033.
- Le DT, Uram JN, Wang H, Bartlett BR, Kemberling H, Eyring AD, *et al.* PD-1 blockade in tumors with mismatch-repair deficiency. *N Engl J Med* 2015;372:2509–2520. doi: 10.1056/NEJMoa1500596.
- Roach C, Zhang N, Corigliano E, Jansson M, Toland G, Ponto G, *et al.* Development of a companion diagnostic PD-L1 immunohistochemistry assay for pembrolizumab therapy in non-small-cell lung cancer. *Appl Immunohistochem Mol Morphol* 2016;24:392–397. doi: 10.1097/PAL.0000000000000408.
- Alexandrov LB, Nik-Zainal S, Wedge DC, Aparicio SA, Behjati S, Biankin AV, *et al.* Signatures of mutational processes in human cancer. *Nature* 2013;500:415–421. doi: 10.1038/nature12477.
- Pfeifer GP. Mutagenesis at methylated CpG sequences. *Curr Top Microbiol Immunol* 2006;301:259–281. doi: 10.1007/3-540-31390-7_10.
- Swanton C, McGranahan N, Starrett GJ, Harris RS. APOBEC enzymes: mutagenic fuel for cancer evolution and heterogeneity. *Cancer Discov* 2015;5:704–712. doi: 10.1158/2159-8290.CD-15-0344.
- Cancer Genome Atlas Network. Comprehensive molecular characterization of human colon and rectal cancer. *Nature* 2012;487:330–337. doi: 10.1038/nature11252.
- Kandoth C, Schultz N, Cherniack AD, Akbani R, Liu Y, *et al.* Cancer Genome Atlas Research Network. Integrated genomic characterization of endometrial carcinoma. *Nature* 2013;497:67–73. doi: 10.1038/nature12113.
- Rizvi NA, Hellmann MD, Snyder A, Kvistborg P, Makarov V, Havel JJ, *et al.* Cancer immunology. Mutational landscape determines sensitivity to PD-1 blockade in non-small cell lung cancer. *Science* 2015;348:124–128. doi: 10.1126/science.aaa1348.
- McGranahan N, Furness AJ, Rosenthal R, Ramskov S, Lyngaa R, Saini SK, *et al.* Clonal neoantigens elicit T cell immunoreactivity and sensitivity to immune checkpoint blockade. *Science* 2016;351:1463–1469. doi: 10.1126/science.aaf1490.
- Boland CR, Goel A. Microsatellite instability in colorectal cancer. *Gastroenterology* 2010;138:2073–2087.e3. doi: 10.1053/j.gastro.2009.12.064.
- Nakazato H, Takeshima H, Kishino T, Kubo E, Hattori N, Nakajima T, *et al.* Early-stage induction of SWI/SNF mutations during esophageal squamous cell carcinogenesis. *PLoS One* 2016;11:e0147372. doi: 10.1371/journal.pone.0147372.
- Oike T, Ogiwara H, Nakano T, Yokota J, Kohno T. Inactivating mutations in SWI/SNF chromatin remodeling genes in human cancer. *Jpn J Clin Oncol* 2013;43:849–855. doi: 10.1093/jcco/hyt101.
- Wu RC, Wang TL, Shih IM. The emerging roles of ARID1A in tumor suppression. *Cancer Biol Ther* 2014;15:655–664. doi: 10.4161/cbt.28411.
- Yoshida M, Yokota E, Sakuma T, Yamatsuji T, Takigawa N, Ushijima T, *et al.* Development of an integrated CRISPRi targeting Δ Np63 for treatment of squamous cell carcinoma. *Oncotarget* 2018;9:29220–29232. doi: 10.18632/oncotarget.25678.
- Mullighan CG, Zhang J, Kasper LH, Lerach S, Payne-Turner D, Phillips LA, *et al.* CREBBP mutations in relapsed acute lymphoblastic leukaemia. *Nature* 2011;471:235–239. doi: 10.1038/nature09727.
- Gui Y, Guo G, Huang Y, Hu X, Tang A, Gao S, *et al.* Frequent mutations of chromatin remodeling genes in transitional cell carcinoma of the bladder. *Nat Genet* 2011;43:875–878. doi: 10.1038/ng.907.
- Bertoli C, Skotheim JM, de Bruin RA. Control of cell cycle transcription during G1 and S phases. *Nat Rev Mol Cell Biol* 2013;14:518–528. doi: 10.1038/nrm3629.
- Makohon-Moore A, Iacobuzio-Donahue CA. Pancreatic cancer biology and genetics from an evolutionary perspective. *Nat Rev Cancer* 2016;16:553–565. doi: 10.1038/nrc.2016.66.
- Dickson MA, Schwartz GK, Keohan ML, D'Angelo SP, Gounder MM, Chi P, *et al.* Progression-free survival among patients with well-differentiated or dedifferentiated liposarcoma treated with CDK4 inhibitor Palbociclib: a phase 2 clinical trial. *JAMA Oncol* 2016;2:937–940. doi: 10.1001/jamaoncol.2016.0264.
- Kojima T, Shah MA, Muro K, Francois E, Adenis A, Hsu CH, *et al.* Randomized phase III KEYNOTE-181 study of pembrolizumab versus chemotherapy in advanced esophageal cancer. *J Clin Oncol* 2020;38:4138–4148. doi: 10.1200/JCO.20.01888.
- Greally M, Ku GY. Immune checkpoint inhibitors in esophagogastric adenocarcinoma: do the results justify the hype? *J Thorac Dis* 2018;10:6407–6411. doi: 10.21037/jtd.2018.12.01.
- Matsumoto Y, Nagasaka T, Kambara T, Hoshizima N, Murakami J, Sasamoto H, *et al.* Microsatellite instability and clinicopathological features in esophageal squamous cell cancer. *Oncol Rep* 2007;18:1123–1127.
- NCCN Clinical Practice Guidelines in Oncology. Esophageal and Esophagogastric Junction Cancers v.1; 2019. Fort Washington: National Comprehensive Cancer Network (NCCN); 2019. Available from: https://www.nccn.org/professionals/physician_gls/default.aspx#esophageal. [Accessed March 20, 2019]
- Singal G, Miller PG, Agarwala V, Li G, Kaushik G, Backenroth D, *et al.* Association of patient characteristics and tumor genomics with clinical outcomes among patients with non-small cell lung cancer using a clinicogenomic database. *JAMA* 2019;321:1391–1399. doi: 10.1001/jama.2019.3241.
- Kim YB, Ahn JM, Bae WJ, Sung CO, Lee D. Functional loss of ARID1A is tightly associated with high PD-L1 expression in gastric cancer. *Int J Cancer* 2019;145:916–926. doi: 10.1002/ijc.32140.

How to cite this article: Wang L, Jia YM, Zuo J, Wang YD, Fan ZS, Feng L, Zhang X, Han J, Lyu WJ, Ni ZY. Gene mutations of esophageal squamous cell carcinoma based on next-generation sequencing. *Chin Med J* 2021;134:708–715. doi: 10.1097/CM9.0000000000001411